



First-Principles Simulations of Biological Molecules Subjected to Ionizing Radiation

Karwan Ali Omar, Karim Hasnaoui, Aurélien de La Lande

► To cite this version:

Karwan Ali Omar, Karim Hasnaoui, Aurélien de La Lande. First-Principles Simulations of Biological Molecules Subjected to Ionizing Radiation. *Annual Review of Physical Chemistry*, 2021, 72 (1), pp.445-465. <10.1146/annurev-physchem-101419-013639>. <hal-03456039>

HAL Id: hal-03456039

<https://hal.science/hal-03456039v1>

Submitted on 30 Jan 2024

HAL is a multi-disciplinary open access archive for the deposit and dissemination of scientific research documents, whether they are published or not. The documents may come from teaching and research institutions in France or abroad, or from public or private research centers.

L'archive ouverte pluridisciplinaire **HAL**, est destinée au dépôt et à la diffusion de documents scientifiques de niveau recherche, publiés ou non, émanant des établissements d'enseignement et de recherche français ou étrangers, des laboratoires publics ou privés.



HAL Authorization

First-Principles Simulations of Biological Molecules Subjected to Ionizing Radiation

Karwan Ali Omar^{1,2}, Karim Hasnaoui^{3,4}, Aurélien de la Lande^{1*}

1. Institut de Chimie Physique, Université Paris-Saclay, CNRS, UMR 8000. Orsay, France.
2. Department of Chemistry, College of Education, University of Sulaimani, 41005, Kurdistan, Iraq.
3. Institut du Développement et des Ressources en Informatique Scientifique, rue John von Neumann, B.P. 167, 91403, Orsay, France.
4. Université Paris-Saclay, UVSQ, CNRS, CEA, Maison de la Simulation, 91191, Gif-sur-Yvette, France.

*To whom correspondence should be addressed: aurelien.de-la-lande@universite-paris-saclay.fr

Keywords: radiation chemistry, first-principles simulations, RT-TD-DFT, charge migration, radical chemistry.

Abstract:

Ionizing rays cause deleterious damage to genomes, proteins and signaling pathways that normally regulate cell activity, with harmful consequences such as accelerated ageing, tumors and cancers, but also with beneficial effects in the context of radiotherapies. They may either be high-energy photons (XUV-rays, X-rays, γ -rays) or charged particles (H^+ , He^{2+} , e^- , $\mu^- \dots$). While the great pace of research in the XXth century led to the identification of the molecular mechanisms for chemical lesions on the building blocks of biomolecules, the last two decades have brought renewed questioning, for example, regarding the formation of clustered damages or the rich chemistry involving the secondary electrons produced by radiolysis. Radiation chemistry is now meeting attosecond science, providing extraordinary opportunities to unravel the very first stages of biological matter radiolysis. The situation calls for first-principles numerical approaches to simulate the multiscale responses of biological matter subjected to ionizing radiation (IoR) to help and complement the interpretation of experimental data. This review provides an overview of the recent progress made in this direction, focusing mainly on the atto- to femto- to picosecond time

scales. We review, in particular, promising applications of Time-Dependent Density Functional Theory to address the first stage of radiolysis in realistic models.

INTRODUCTION

The discovery that high-energy radiation has major physiological effects dates back to the early days of radioactivity. In her PhD thesis (1), Marie Curie reviewed the observations of Walkhoff, Giesel, Becquerel and P. Curie that skin exposure to radium causes red blotches or even blisters in case of longer exposures, noting in the meantime the first attempts made at the Saint-Louis hospital in Paris to use radium-emitted rays to cure skin diseases. She also mentioned the deleterious action of the rays produced by radium on plant leaves that turn yellow and become friable. She further reported the observations from Giesel that development of macrobian populations is slowed down upon exposure to radium, although moderately. 120 years later, we know that the radiation emitted by radioactive elements (α or β^- particles) or X-rays, is ionizing radiation (IoR). IoR interact so strongly with the electron cloud of molecules composing the cell, that they induce their ionizations. Energy deposition triggers a cascade of physical-chemical events that lead to the formation of chemical lesions on essential-for-life biomolecules such as DNA, proteins and lipids. The terminology IoR actually refers to a wider family of particles, encompassing both high-energy photons (eXtreme Ultraviolet XUV-rays, X-rays or γ -rays) and charged particles (e.g. atom nuclei, electrons, positrons, muons...) in the keV-MeV kinetic energy range (2).

IoR has either natural (rocks, seas, sun, cosmos) or anthropogenic origins (medicine, nuclear-plant wastes, nuclear-plant disasters, nuclear-weapon testing). The exposure of the human body to IoR is deleterious as radiation damages induced by IoR cause metabolic dysfunctions, accelerated ageing and contribute to the appearance of cancerous tumors(3). DNA has been considered for a long time as the main macrobiomolecule to consider to account for the physiological consequences of irradiation (3). This makes sense because DNA is at the core of the genetic information storage system. Without minimizing the importance of DNA though, evidence has accumulated that irradiation of other cellular machineries, for instance mitochondria in Eukarotic cells (4–6), ion channels(7), or cellular structures like lipid layers (8), also contribute to the cellular responses to irradiation.

Astronauts placed beyond the Earth's magnetosphere, are subjected to intense solar and cosmic rays (composed of a majority of 1 MeV protons, but also of heavier elements). This represents a major issue for future space exploration *e.g.* to envision Moon colonization or the exploration of Mars by humans (9).

Besides these deleterious effects, we mention the strategies devised by physicians to harvest the devastating power of IoR in so-called radiotherapeutic treatments aimed at killing cancer cells. At the dawn of the XXIst century, particle therapies relying on protons or on heavier atomic nuclei (*e.g.* C⁶⁺), eventually coupled to the use of radiosensitizers (10), are renewed radiotherapies that should permit more controlled dose delivery, hence alleviating the risks of irradiating the surrounding healthy tissues (11, 12). One can logically expect that detailed knowledge of damage formation at the molecular level will help to unravel the molecular basis of particle therapies and contribute to their development.

A main current topic of research remains the formation of clustered damages formed along the particle tracks (13–15). Clustered damages are associated with base excision, DNA/DNA or DNA/histones cross-links, single and double strand breaks. When formed in too dense clusters, DNA becomes difficult, if not impossible, to repair by the cell (16, 17). They can also modify epigenetic regulation of gene expression if key chemical functionalizations on histone are altered (18, 19). Their molecular mechanisms of formation largely await discovery.

Pioneering experiments by Sanche and co-workers combining irradiation by external electron sources with well-controlled kinetic energies (1.8 to 20 eV) and chemical analyses of the degradation products, have revealed the ability of low-energy electrons (LEE) to induce damage on DNA and peptides(20–22). The underlying mechanisms start by electron attachment within shape or core-excited Feshbach resonances (21), followed by energy redistribution into vibrational modes, eventually leading to bond breaking. While the studies in the Sanche laboratory were carried out on solid-state samples, the first evidence of the reactivity of the pre-solvated electron in the liquid phase has been reported comparatively recently(23, 24). For example, Mostafavi and co-workers reported different reactivity for the “near-free” electron *vs.* solvated electron with uracil monophosphate, showing that only the former induces bond breaking between the base and

the ribose. These data probe the production, the diffusion and the reactivity of LEE in natural biological structures. This is another front that should stimulate active research in the near future. We wish to mention two other research areas where IoR is thought to be a central player. One is interstellar chemistry. Several on-going projects aim at clarifying the role of IoR in the formation of pre-biotic molecules on comets or icy grains(25), and also, presumably, in the atmospheres of Jupiter and Saturn's natural satellites (26). The other one is biomolecular 3D imaging by X-ray diffraction techniques. X-ray photon beams induce radiation damage during data record(27). Research is, for example, on-going to determine the location and chemical composition of damages within DNA/protein complexes(28). The recent advent of Extreme Free Electron Lasers that reduce drastically the duration of sample exposure alleviate this risk, but no definitive solution seems to have yet been reached in the community of crystallographers (27)

We finally stress the extraordinary opportunities that are emerging from the development of attosecond or ultrafast spectroscopies(29–31). While traditional time-resolved pulsed radiolysis using beams of charged particles has been essentially limited to the picosecond regime, see e.g. (32), leaving a thick veil on the physical chemistry taking place at earlier times, attosecond sciences are clearly changing the situation. For example, the measurement of one of the earliest chemical events in water radiolysis ($\text{H}_2\text{O}^{*+} + \text{H}_2\text{O} \rightarrow \text{HO}^\bullet + \text{H}_3\text{O}^+$) could be recently time-resolved for the first time by using tunable femtosecond soft x-ray pulses from an X-ray free electron laser (29). Other studies led to proposed new reaction channels leading to the formation of dicationic water clusters by Intermolecular Coulomb Decay (33). These first studies doubtlessly pave the way toward exciting discoveries in the coming years.

Theory and computer modelling have been mobilized for many years to help the interpretation of experimental data and excellent reviews have been published (34–38). The great variety of methodologies developed in the field cannot be summarized here. We instead adopt a complementary perspective and paint a state-of-play of the first-principles approaches dedicated to molecular simulations of the radiolysis of biological matter. Most importantly, we attempt to pinpoint the current methodological roadblocks that, from our point of view, will need to be overcome. We make the arbitrary choice to focus on first-principles methodologies that capture the dynamics of the phenomena at play in the formation of radiation damage. We have decided to

focus on the first stages of radiolysis of biological matter, covering energy deposition to ultrafast chemistry, for which important progress has been made in recent years. We may occasionally borrow examples of applications from related fields, like material science.

1. Hallmarks of radiation chemistry

Following IUPAC, we make a clear distinction between radiation chemistry and photochemistry. Admittedly, both deal with chemical reactivity involving electronic excited states, and, in biology, can lead to severe damage to biomolecules. On the other hand, the initial excitation is very different, and consequently triggers different physical-chemical responses. In photochemistry one usually deals with long duration light pulses having well-defined energies of at most a few eV. Irradiation vibrationally or electronically excites molecules selectively, populating in general one given excited state. We illustrate the case of radiation chemistry, considered in Figure 1, a large biological architecture subjected to irradiation by a charged projectile. The central image depicts a nucleosome, an assembly of a 146-base-pair DNA double strands wrapped around a core made of eight histone proteins. Charged particles interact with matter by Coulomb scattering. Projectiles of kinetic energy in the keV-MeV energy range mainly interact with electrons along their propagation tracks, impacting mainly valence electrons. The amount of energy deposited can be huge, going up to several tens of eV per molecule (39) and energy deposition is widespread along the projectile track. As the duration of interaction is very short, on the subfemtosecond timescale, collisions produce quantum superpositions involving a large number of electronic excited states (Figure 1, C). IoR produces, by definition, a huge number of low-energy electrons that further irradiate the surrounding matter. γ rays interact with matter via the Compton effect, producing showers of high-energy secondary electrons that ionize surrounding matter. X-rays interact via the photoelectric effect, targeting core-shell electrons. X-ray ionization opens specific evolution channels involving for instance Auger decays (40), Intermolecular Coulomb Decays (41).

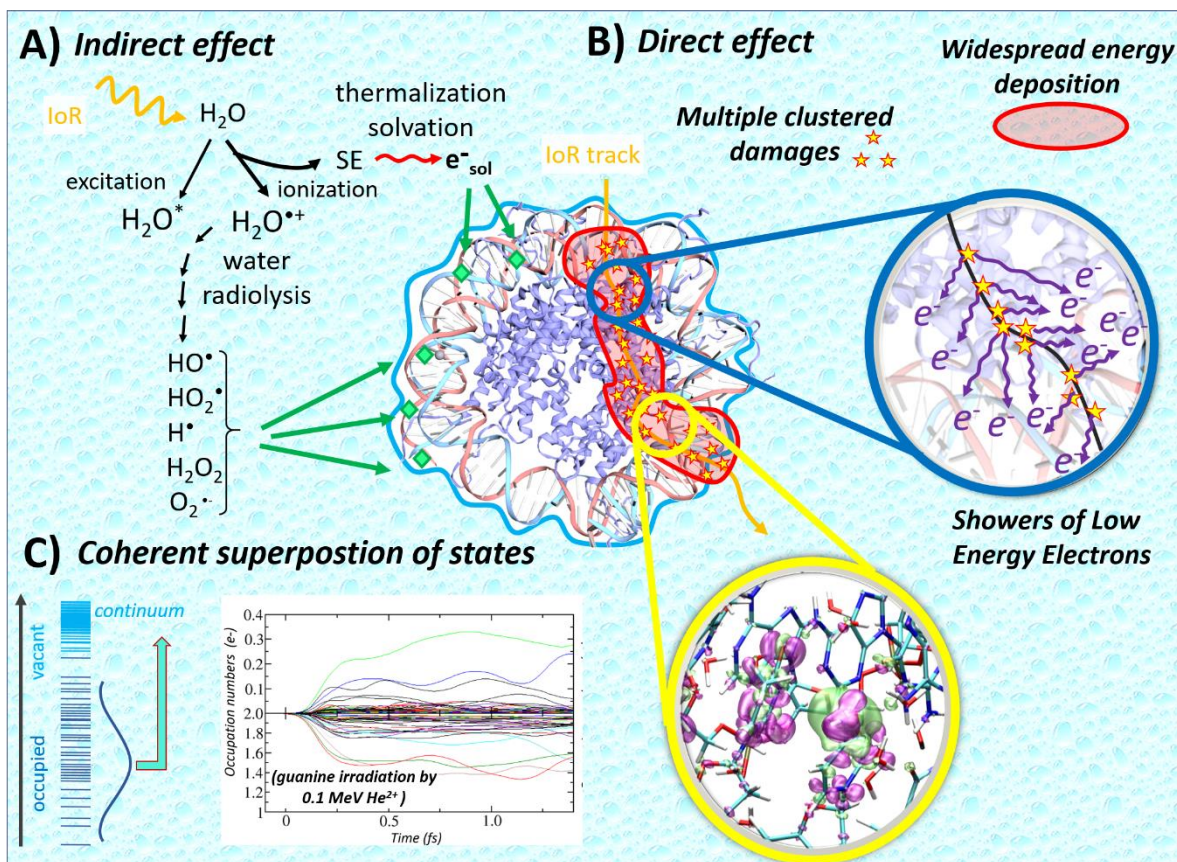


Figure 1: The hallmarks of IoR irradiation, illustrated in the case of a nucleosome - a 12 nm width assembly of DNA wrapped around a core of histone proteins – irradiated by a charged particle (α , β , μ ...) . A) Water radiolysis produces ROS and solvated electrons that attack biomolecules after diffusion (indirect effect). B) Direct irradiation on the nucleosome induces widespread energy deposition (red zone) with copious emission of low energy electrons, and ultimately formation of dense multiple clustered damages. C) An attosecond collision of DNA base by a 0.1 MeV α particle produces a superposition of quantum states; this is reflected by many initially occupied molecular orbitals that get partially depopulated, while populating several vacant orbitals; adapted from Ref. (39).

Damages triggered by IoR have been customarily classified as stemming from indirect or direct effects (Figure 1, A vs. B). The indirect effect refers to damages initiated by water radiolysis ($\text{H}_2\text{O} \rightarrow \text{H}_2\text{O}^+ + 1e^-$) which produces reactive oxygen species that diffuse before attacking a wide variety of chemical functions on biomolecules(42). Direct damages are caused by energy deposition in the biomolecules themselves(43). For the sake of completeness, we further mention the quasi-direct effect proposed by Sevilla and co-workers in the 1990s(44) to describe ultrafast charge transfer between DNA, and by extension other biomolecules, with H_2O^+ produced by irradiation in the first hydration shell of biomolecules (*e.g.* $\text{DNA} + \text{H}_2\text{O}^+ \rightarrow \text{DNA}^+ + \text{H}_2\text{O}$).

The responses of matter subjected to IoR are truly multiscale (Figure 2) and have been customarily classified according to the kind of processes involved in the successive temporal sequences. The definition and the borders between successive stages are of course arbitrary, but this classification helps to set up ideas. The physical stage refers to the deposition of energy, to electronic excitations, ionizations and other purely electronic processes (Intermolecular Coulomb Decay(41), charge migration(45), Auger Decay, energy relaxation and dissipation ...). One can position the end of the physical stage when nuclear response starts to be significant, thereby entering the physical-chemistry stage. Within a few picoseconds, a very complex non-adiabatic dynamics coupling electronic to nuclear motion can lead to fragmentations, molecular explosions or the production of a myriad of chemically harsh radicals. The attachment of low-energy electrons to biomolecules also takes place during the physical-chemical stage. Once the dust has started to settle, a chemical reactivity taking place under thermodynamic equilibrium governs the formation of damages to biomolecules. The biological stage finally refers to the consequences for the structure and for dynamics of damaged biological molecules. It also covers the metabolic responses of the cell, which includes, non-exhaustively, the detection and reparation of DNA damage by the cellular machinery, some epigenetic responses, as well as adaptation of the energy machineries (mitochondria).

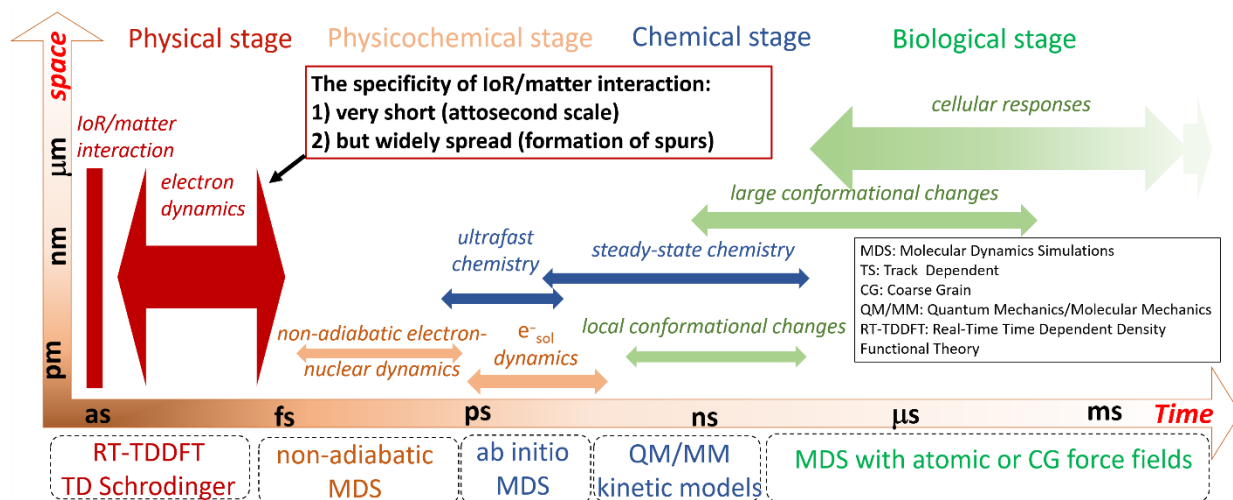


Figure 2: Interaction of IoR with biological matter induces multiscale responses in time and spaceIn the bottom we indicate, not exhaustively, some of the methodologies found in the literature to address the different scales.

This sketchy description of the multiscale responses of biomolecules irradiated by IoR will guide us in the next section. Common methods found in the literature to simulate the physical and

physical-chemical stages are Monte Carlo track structure (MCTS) algorithms(46, 47). MCTS rely on sets of parametrized elementary cross sections (excitation/ionization, electron scattering, electron attachment...) to simulate stochastically the succession of physical and physical-chemical events in the medium. Although valuable to deal with homogenous media, these approaches face insurmountable hurdles with the staggering number of events to parametrize for biological molecules, especially in terms of chemical reactions. Some chemical reactions may also turn out to be impossible to identify and to be parametrized in advance. Furthermore, MCTS rely on important hypotheses (e.g. transferability of the parameters, static description...) that are hardly justified for highly heterogenous biological systems. First-principles methodologies thus represent valuable alternatives, as discussed in the next Section.

2. FIRST-PRINCIPLES SIMULATIONS OF THE PHYSICAL STAGE

2.1 Electron dynamics simulations

Simulating the physical stage is challenging as the objective is to capture strong electronic excitations in large molecular systems, with emission of electrons into the continuum. The “good old quantum chemistry toolbox” that deals with electrons bound to molecule is not directly usable. Wave functions for electrons in the continuum are delocalized and exhibit oscillatory behavior that is not easily captured by standard basis sets. The choice of a particular methodology is generally guided i) by the nature of the ionizing radiation which determines the kind of initial excitation to be modelled as well as the subsequently available evolution channels and, ii) the tradeoff between accuracy and computational cost and the level of accuracy one is willing to sacrifice. Some authors working in the field of attosecond science proposed to combine Gaussian basis functions to describe bound electrons with B-splines to describe electrons in the continuum(48). Excellent agreement could be obtained with such schemes to reproduce experimental cross-sections of Ne photoionization and application to medium sized molecules are on the way. The treatment of resonances is another difficult task to address. To this end, Krylov and co-workers have extended the equation-of-motion coupled cluster method to the use of complex absorbing potentials (CAP) with promising applications (49). A dedicated scheme using configuration interaction has been developed to capture Fano resonances (50). Progress has been made too in the context of Density Functional Resonance Theory (51).

For the treatment of large and realistic molecular models, simulations based on Time-Dependent Density Functional theory (TD-DFT) (52) represent a workhorse. To simulate the physical stage one can simulate step-by-step the response of the electronic cloud subjected to a perturbation by discretizing time into small time steps, typically of a few attoseconds and by propagating TD-DFT equations (53, 54). Within the Kohn-Sham framework, the basic equation-of-motion reads:

$$i \frac{\partial \rho(\mathbf{r}, t)}{\partial t} = [H(\mathbf{r}, t), \rho(\mathbf{r}, t)] \quad (1)$$

$$H(\mathbf{r}, t) = T_s[\rho(\mathbf{r}, t)] + v_{ee}[\rho(\mathbf{r}, t)] + v_Z + v_{IoR} \quad (2)$$

where T_s is the kinetic energy functional of the Kohn-Sham non-interacting electron gas, v_Z and v_{ee} are the potential created by the atomic nuclei and by the electron cloud respectively, v_{xc} is the exchange-correlation potential. v_{IoR} is the potential created by the IoR.

For photon irradiation, a classical dipole approximation is often assumed by which the electronic system interacts with the electric field component of the electromagnetic light (\mathbf{F}_{IoR} , bold characters indicate vectors) through its molecular dipole, *i.e.* $v_{IoR} = \mathbf{F}_{IoR} \cdot \mathbf{d}$. The mathematical form of \mathbf{F}_{IoR} can be shaped to mimic specific light sources, like continuous light or a Gaussian electric pulse. A more realistic description of photon-electron interaction came recently with an approach bridging DFT and quantum electrodynamics(55). This promising approach treats on equal footing the photon and the electrons at the quantum level of description.

Charged particles interact with matter via the Coulomb interaction. For heavy projectiles (H^+ , He^{2+} or other heavier ions), a classical representation can be adopted and v_{IoR} is conveniently calculated from a relativistic Liénard-Wiechert formula (56). For lighter projectiles, notably electrons, the situation is more delicate as one can hardly ignore the quantum nature of the projectile. We are not aware of methodologies described in the literature to simulate such irradiation by RT-TD-DFT. Rizzi et al. attempted to simulate electron injection into small water chains, comparing two methodologies; one using an electron pulse and another a steady stream of electrons (57). They highlighted the difficulties of controlling injection conditions, but they paved the way for future more realistic simulations. Some help might also come from conceptual developments within the exact factorization formalism(58) or from multicomponent DFT(59).

Having set up the Kohn-Sham Hamiltonian, accurate and stable algorithms are available to propagate TD-DFT equations (60, 61). Computer codes for RT-TD-DFT have flourished in the last two decades, some with impressive performance in terms of system size (62–64). We have on our side developed a RT-TD-DFT implementation within the context of Auxiliary DFT (ADFT)(65). ADFT uses variational density fitting (66) to substitutes in a controlled manner, the electron-repulsion potential and the XC potential computed directly from Kohn-Sham orbitals by quantities evaluated from fitted densities developed over mono-centric basis functions. An advantage of the local basis set ansatz used in deMon2k(67) is that hybrid or range-separated XC functionals that incorporate a fraction of exact exchange remain tractable even for large molecular systems (68, 69). A further advantage of ADFT comes from the possibility to carry-out repetitive on-the-fly analyses of the time-dependent electronic structure without introducing supplementary computational cost (70). Figure 3 illustrates the computational performances of our current CPU-based (Central Processing Units) implementation. The four most computationally demanding tasks are highlighted, among which matrix exponential evaluations are the most demanding one and require optimized libraries such Scalapack to remain efficient. Note also the low computational cost and remarkable scaling of Kohn-Sham (KS) potential evaluations that is permitted by ADFT. To go larger and to tackle the molecular complexity of biological systems, we have developed a hybrid scheme coupling RT-TD-ADFT to polarizable Amber ff02 Molecular Mechanics force field (71, 72). Our implementation includes retardation in the electric field propagation that mediates the polarization of the two regions (56).

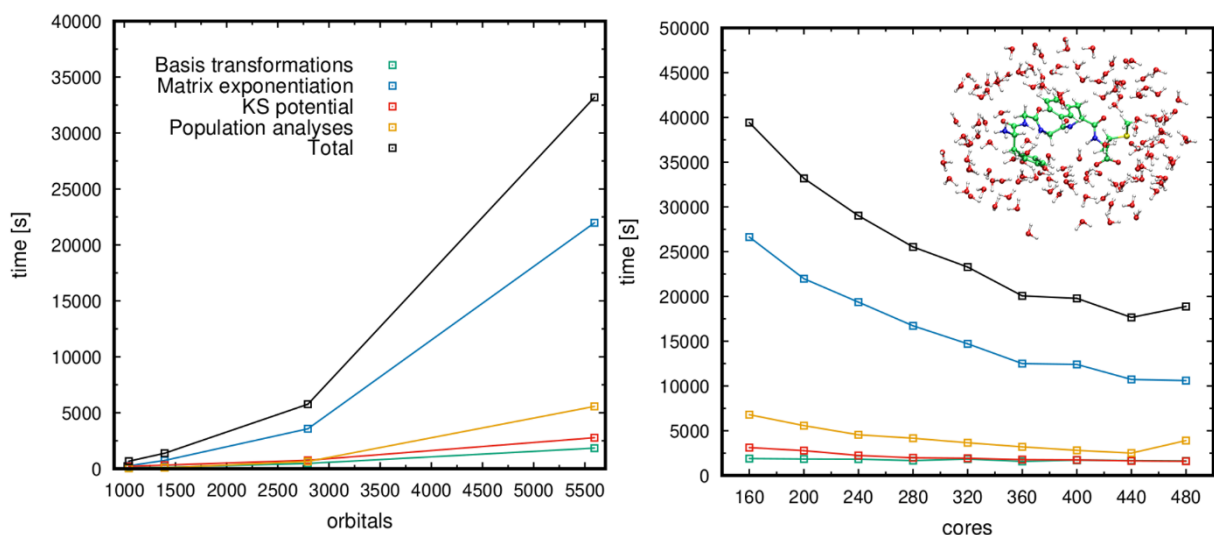


Figure 3: Computational performances of RT-TD-ADFT in deMon2k taking the example of a solvated metenkephalin. The simulation consists in 200 as electron dynamics simulation (1 as time step with a predictor-corrector scheme), extracting atomic charges at every time step. Right: computational cost as a function of the thickness of the solvation layer (from 0 to 6 Å) and reflected by the number of atomic orbitals. Left: scaling performances with the number of computer cores for the 6 Å solvation layer.

Electron dynamics simulations can either be carried out at fixed nuclear position (so-called purely RT-TD-DFT simulations), but nuclear motion can be straightforwardly coupled via the Ehrenfest MD approach (73, 74). In that case, atomic nuclei are assumed to move according to Newton's law ($\mathbf{F}_A = m_A \cdot \mathbf{a}_A$, the three terms being the force acting on nucleus A, its mass and its acceleration) and calculating the forces acting on the nuclei directly from the average potential energy provided by RT-TD-DFT, namely $\mathbf{F}_A = \partial E[\rho(t)]/\partial \mathbf{R}_A$. Ehrenfest MD opens the way to the simulation of both the physical and physical-chemical stages. Examples of applications will be given in Section 3.

2.2 Electronic Stopping Power Calculations with RT-TD-DFT

The stopping power (SP) is a property characterizing energy deposition by a projectile in matter as a function of the kinetic energy of the projectile. It is defined as the derivative of the total potential energy with respect to the projectile displacement(75). As a consequence of the mass difference between atom nuclei and electrons, that both interact with charged projectiles, the total stopping power can be decomposed to a good approximation into a nuclear and an electronic component. Both exhibit a concave shape but with different maximum positions. Nuclear SP dominates over electronic SP at low kinetic energy (<0.01 MeV/nuc), while electronic SP are predominant between 0.01 and a few hundreds of MeV/nuc. Electronic stopping power for many projectile types and materials have been measured for decades and collected in data banks available on line(76, 77). They are sometimes complemented by semi-empirical data obtained by application of analytical models like Bethe's theory (78). The electronic stopping power is thus an ideal target property to assess the reliability of RT-TD-DFT to simulate energy deposition by charged projectiles. Overall, the results obtained by various groups so far are encouraging (75, 79–81). First, calculated electronic stopping power curves have been found to be of similar shape and amplitude as the experimental curves for projectiles in the keV-MeV kinetic energy range. On the other hand, a conclusion emerging from various studies is a marked sensitivity of SP with the basis set(80, 82). The pressure put on the basis set quality depends on the energy region in which one is

interested. Around the SP maximum, a good description of valence electrons is mandatory while at high projectile energies, contributions from core excitations must be properly considered (82). SP calculations seem to be weakly sensitive to exchange-correlation effects. The simplest Local Density Approximation already provides similar results to Generalized Gradient Approximation (GGA) or hybrid GGA XC functionals (53). This can be understood by the fact that energy deposition is essentially driven by Coulomb interactions and marginally by XC effects. Even though encouraging, a more in-depth understanding of this finding is needed. In fact, most LDA or GGA functionals are known to inadequately position Rydberg or charge-transfer states and notably underestimate ionization potentials (83). Thus, even though the densities of states generated by different functionals give similar energy depositions, the nature of the populated excited states might be drastically different. If so, the subsequent dynamics might be XC-functional-dependent, eventually producing irrelevant charge-migration mechanisms. We also note that previous simulations have been carried out under the adiabatic approximation. The latter consists in ignoring explicit time dependence of the XC potential ($v_{xc}[\rho(\mathbf{r}, t)] \rightarrow v_{xc}[\rho(\mathbf{r})]$). As irradiation can be accompanied by abrupt variations of the electron density with compressions or dilations(84, 85), XC functionals incorporating memory and dissipation effects might be mandatory (86). Nonetheless, the first applications of RT-TD-DFT stopping power calculations are encouraging for applications of the methodology to biological models.

2.3. Electron Dynamics Simulations in Biomolecules

Water is probably worth considering as a prime biological molecule. Privett et al investigated the one-electron transfer from water clusters containing from one to six molecules, to 0.1 MeV H^+ (87). They employed a “simplest-level-electron nuclear dynamics method” and found qualitative agreement with available experimental cross-sections for the smallest clusters. Keeves and Kanai reported purely RT-TD-DFT-based stopping power calculations on systems comprised of 162 water molecules with periodic boundary conditions to mimic bulk water. They found the formation of the water cation (H_2O^+), finding that excitations primarily involve oxygen lone pairs (88).

The advantage of DFT-based approaches is the lower computational cost that permits the investigation of large molecular systems. Kanai and co-workers reported stopping power calculations in DNA for helium and hydrogen nuclei (89). The simulations were carried out on 10

base pairs DNA (CGCGCTTAAG sequence) in the gas phase, encompassing 684 atoms and 2,220 electrons. They compared the electronic SP for collision trajectories perpendicular to the DNA double strand to a perturbative treatment based on the Born approximation. Encouraging agreement was found between the two approaches. The authors analyzed hole formation, highlighting the contributions of high-lying occupied Kohn-Sham MOs to the ionization process. Interestingly, they further showed that hole production did not correlate directly with energy deposition, as generally thought. Instead maximum hole production was obtained for projectile energies lower than the Bragg peak. The origin of this difference is yet to be fully clarified.

We investigated the ionization mechanism triggered by H^+ , He^{2+} and C^{6+} ions traversing a solvated DNA double strand by means of a hybrid RT-TD-ADFT/MM approach (7 base pairs and 99 solvation water molecules for a total of 742 atoms and 3,170 electrons were described at the DFT level, see Figure 4, A) (90). The projectile successively struck seven molecular moieties. We revealed an ebb-and-flow ionization mechanism. As the incoming projectile is positively charged, it strongly polarizes the electron cloud when approaching a molecule, dragging the density to it (B). Immediately after collision, the electrons flow back and a fraction of the electron density is emitted. The slower the projectile, the larger the amplitude of flow/back flow of the density (90). To which extent this so-called ebb-and-flow ionization mechanism influences energy deposition and ionization probabilities remains to be clarified, but this is another example of a process only accessible by electron dynamics simulations. We found that ionization takes place in less than a few hundreds of attoseconds, independently of the projectile charge, but depending, as expected, on the projectile speed. We further investigated subsequent charge migrations, showing that holes created on the DNA base delocalize over the riboses in a few femtoseconds (Figure 4, C). On the other hand, similar to the conclusion of Kanai and co-workers, we found that holes don't migrate far away from the sites of formation. Last but not least, we identified the sites of localization of the secondary electrons. They sit on surrounding sugar-base moieties and also on the solvation layer. These findings can be helpful to understand the subsequent reactivity of low energy electrons (see below). Note that the two studies above employed GGA functionals that are known to be plagued by self-interaction-error. This probably affects charge migration mechanisms and will have to be investigated thoroughly.

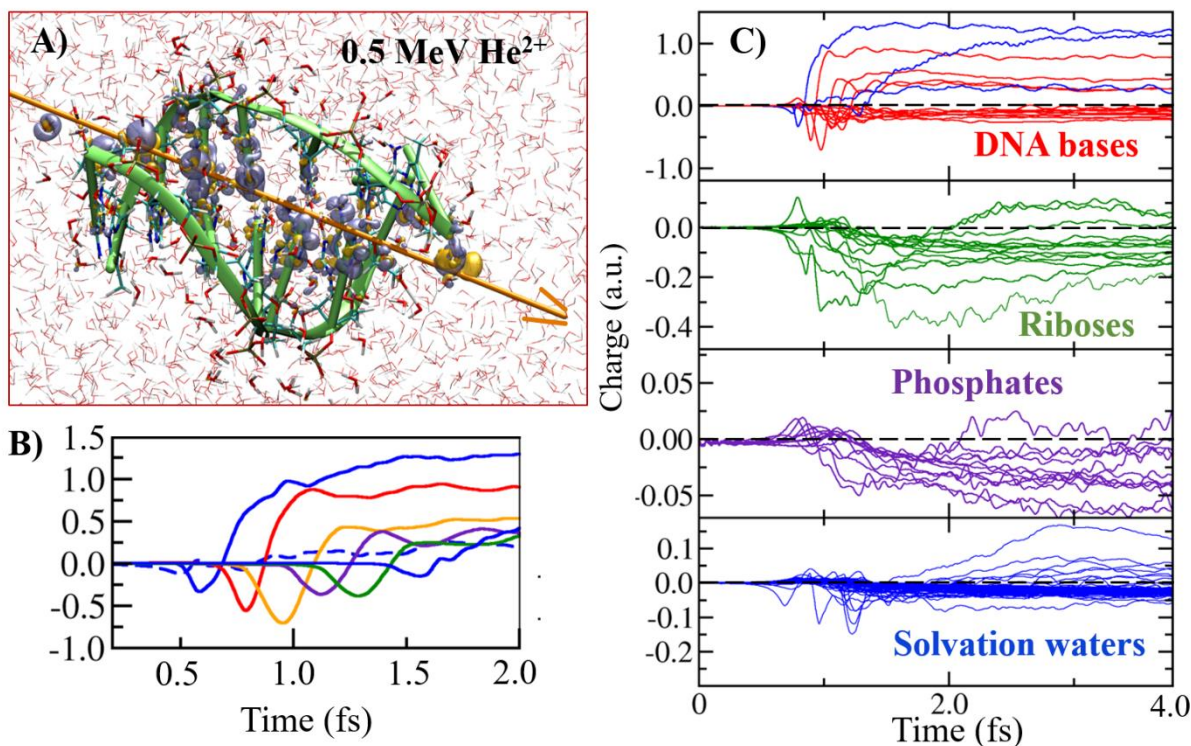


Figure 4: Irradiation of a solvated DNA double strand by a 0.5 MeV He^{2+} ion. A, Isosurface of the deformation electron density just after irradiation. The orange line is the projectile trajectory. B, charge variations of three water molecules (in blue) and four DNA nucleobase (T, C and two GC pairs, respectively in red, orange, violet and green) struck by helium nuclei of different kinetic energy. Just before collision, the fragment accumulates electron density (its charge decreases), before releasing and getting partially ionized. C, Charge fluctuations of all molecular fragments as a function of time. Adapted from Reference (90).

The interplay between charge migration and nuclear motion during the very earliest stage of irradiation is still an open question. On one hand, charge migration between the amine group and the side chain of ionized tryptophan or phenylalanine was shown to be rather insensitive to nuclear motion (31, 91, 92). By comparing RT-TD-DFT simulations with Ehrenfest MD simulations, the authors showed that during the first femtoseconds, nuclear motion had no noticeable effect on the frequencies characterizing charge migration. On the other hand, it was shown that charge migration in a prototypical artificial light-harvesting system was strongly coupled to nuclear vibrations (93). Furthermore, Vacher et al showed, using the direct dynamics variational multiconfigurational Gaussian method, that electronic decoherence causes damping of charge migration already within a few femtoseconds (94). In another study of charge migration within ionized polyene and glycine based on the realization of Ehrenfest MD, some authors showed that dephasing was a major source of decoherence in the first femtoseconds (95). These apparent contradictions tend to indicate that

nuclear motion and electronic decoherence are strongly system-dependent. It is likely that the couplings between the different vibration modes contribute to gate energy flows, hence the response of nuclear wave packets to changes in electron states. The extent to which electronic decoherence impacts the kinds of charge migration in radiation chemistry problems needs to be investigated.

2.4. Challenges for Modelling the Physical Stage

We discuss in this subsection two classes of challenges for the first-principles modelling of radiation chemistry problem that call for methodological developments.

The first kind is caused by other unpleasant consequences of the lack of electronic decoherence. We illustrate three of them in Figure 5, considering very simple systems. In A) we see an irradiation having 10% probability to ionize a water molecule. A mean-field approach like RT-TD-DFT produces an electronic wave packet integrating to $0.1e^-$, not the production of a wave packet integrating to $1e^-$ with 10% probability. This is problematic as a $0.1e^-$ wave packet doesn't have the ionizing properties of a full electron, and if attached to a molecule would only marginally reduce it. In B), the emitted wave packet is equally scattered over three directions, and then further in three. The irradiative properties of scattered electrons becomes somehow diluted. Examples A and B illustrate the failure of standard RT-TD-DFT simulations to deal with the subsequent evolution of secondary electrons produced by irradiation. Case C illustrates another well-known problem of Ehrenfest MD. It shows the radio-induced dissociation of a water molecule provided by Ehrenfest MD. Electronic decoherence is the piece of the puzzle that is missing to recover a phenomenological picture. Many schemes have been proposed from simple patches to sophisticated algorithms (96, 97), they might need adaptation to simulation of the large molecular systems shown for instance in Figure 4A. Recently a development by Wang and co-workers in which decoherence was enforced using information from the adiabatic state populations has been proposed and applied to radiolysis of a small molecule (98).

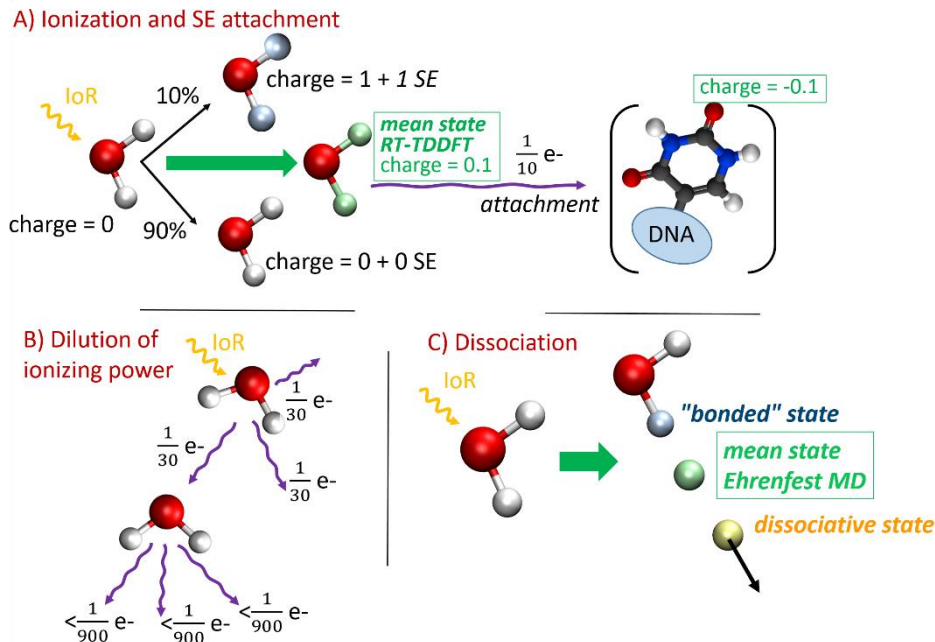


Figure 5: Simple cases to illustrate artefacts caused by lack of electronic decoherence in pure RT-TDFT and Ehrenfest MD. A) A collision with 10% probability of ionization produces a secondary electron wave packet holding 0.1e⁻. Attachment to a DNA base, leads to a species with charge of only -0.1, not -1. B) A collision with 10% probability of ionization produces three negligible wave packets, each having a weak ionizing property. C) If ionization causes a water molecule to dissociate with 50% probability, the Ehrenfest MD trajectory is the fictitious mean "bonded" and "dissociated" molecule.

Another challenge is related to the interpretation and visualization of data produced by simulation algorithms. Radiation chemists are used to employing terms such as single, double ionizations, excitation transfer, amount of deposited energy, kinetic energy of secondary electrons, radicals.... To what extent do the outcomes of RT-TD-DT ED and Ehrenfest MD match this phenomenological description? In the past, theoretical frameworks such as "conceptual DFT(99) or topological analyses(100) were developed by quantum chemists to establish mathematical connections between the outcomes of stationary electronic structure calculations and chemical concepts (chemical bonding, electronegativity, hardness, aromaticity...). A similar effort should probably be made now in the context of non-stationary electron densities to extract comprehensive insights allowing the interpretation of experimental data.

In this direction, we have extended topological analyses to the realm of attosecond electron dynamics(39, 101), considering both the electron density or the time dependent Electron Localization Function(102). As an illustration, Figure 6 shows a water molecule struck by a 10 keV α particle. TD-ELF topological analyses reveal how the projectile is dressed by a wave packet containing 0.8 electron. When applied to larger systems, these analyses reveal a lot of valuable

information on the evolution of the Lewis structure (Right) (39). Much remains to be done though to apply and further develop interpretative tools for electron dynamics simulations.

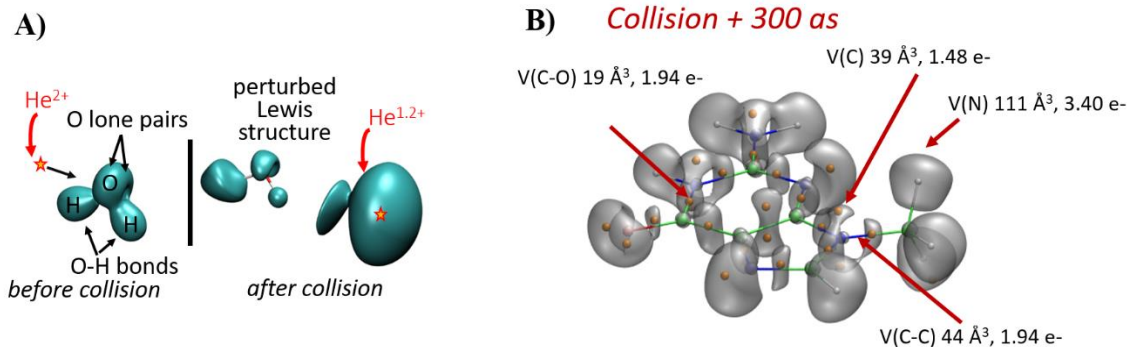


Figure 6: Left, TD-ELF isosurface (0.8) before and after collision of a water molecule by a 10 keV He^{2+} . Right: TD-ELF topological analysis of guanine, 300 as after collision. The analysis reveals the Lewis patterns, in particular a splitting of the central C-C bond. A few selected basins are shown with their volumes and electronic populations. The orange bead are the attractors of the topological basins.

3. DYNAMICS AND REACTIVITY OF LOW ENERGY ELECTRONS

Since the discovery that low energy electrons can induce DNA strand breaks, computer modeling has been used to understand the underlying mechanisms governing their diffusion and their reactivity. The optical properties of the solvated electron were characterized in the 1960' in radiolysis study and the first attempts investigate hydrated electron by numerical simulations date back to the 1980(103). Investigations of deexcitation pathways and the temperature dependent optical properties have been (104).

In 2014, Jungwirth, Hamm and co-workers investigated by transient THz spectroscopy the collapse of a free-electron wavefunction on the femtosecond timescale (105). The authors performed ground-state simulations to investigate the associated time scales. It takes a few hundred femtoseconds for the wave function to collapse and 3 ps to form a solvation cage (Figure 7).

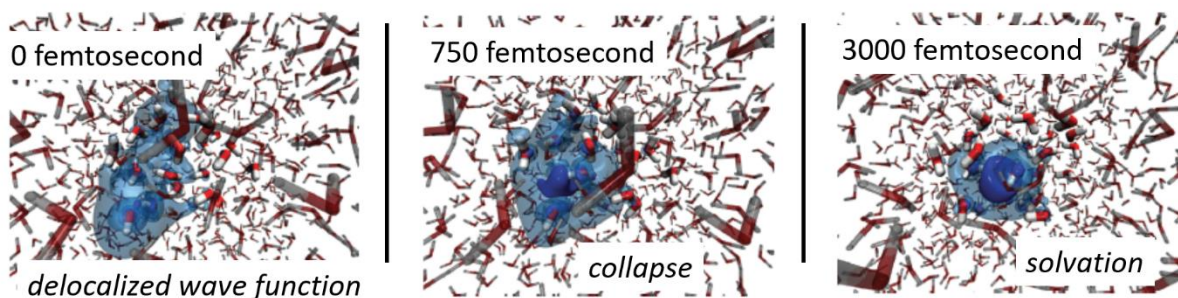


Figure 7: electron wave function collapse and electron solvation after initial excitation. Adapted with permission from Ref. (105).

Lots of studies have addressed the reactivity of LEE with the building block of life, in particular small DNA models. The energetics of LEE induced strand breaks(106–108), base loss(109) or deprotonation have been reported by static approaches relying for instance on DFT. Various excellent recent reviews have been devoted to this topic(35, 110), to which we refer interested readers for more details.

Dynamical approaches have appeared in the last decade. Kumar et al.(110), as well as Smyth and Kohanoff(111) have investigated electron attachment from water to nucleobases by means of ground state Born-Oppenheimer MD simulations (BOMD). Depending on the nucleobase considered this process was shown to take place within 15 fs to a few tens of fs. Dissociative electron attachment in gas phase or environment nucleobases was further investigated by means of BOMD and selected vibrational excitations. McAllister et al. revealed the protective role of waters around the thymine nucleobase, by increasing the barriers to N-H bond breaking(112) They further investigated phosphate-sugar bond breaking nucleotides(35).

In another study, the protecting role of amino-acid residues against the bond breaking of the reduced thymine nucleobase was shown from first-principles simulations (113).

4. ULTRAFAST CHEMICAL REACTIVITY

We finally review in this last section a few examples dealing with the ultrafast chemical reactivity taking place out-of-thermodynamical-equilibrium during the physical-chemical stage. The reactivity of H_2O^{*+} has been the subject of insightful studies. H_2O^{*+} gives a proton to a surrounding water ($\text{H}_2\text{O}^{*+} + \text{H}_2\text{O} \rightarrow \text{HO}^{\cdot} + \text{H}_3\text{O}^+$) presumably in a few tens to a few hundreds of femtoseconds. Recently Loh et al. reported three characteristic times (46 ± 10 fs, 0.18 ± 0.02 ps, and 14.2 ± 0.4

ps) that they assigned to the proton-transfer reaction, to the vibrational cooling of the hot hydroxyl radical and to geminal recombination respectively (29). Non-adiabatic MD simulations combining Hartree-Fock (using Koopmans' theorem to access excited states) with a MM force field to simulate the water environment, led to a characteristic time of 60 fs for the proton transfer, matching reasonably well the experimental 46 fs. In previous simulations carried out with DFT, Marsalek et al. showed that, on the ground state, the hole is delocalized over three water molecules (i.e. $(\text{H}_2\text{O})_3^{*+}$ is a preferable notation to H_2O^{*+}). The amount of exact exchange introduced in the XC functional, to compensate for self-interaction-error, is a crucial parameter that controls the degree of hole delocalization. They found that proton transfer is gated by a preliminary charge re-localization on a single water molecule which takes place in ca. 30fs(114). This is a remarkable example of an “attosecond chemical reaction”; *i.e.* a chemical reaction driven by the electronic motion. More investigation might be needed to compare the reactivities of the radical cation of water in the ground state vs. the excited state, as well as the reactivity in bulk or in the hydration shell of biomolecules. In the latter situation, H_2O^{*+} can act as an oxidant before acting as an acid. This was proven, for example, from experimental/computational studies of pulsed radiolysis of acid solutions (115). Moreover, -Tarif et al. discovered that when H_2O^{*+} is formed in the vicinity of a uracil nucleobase in water, it leads to hydroxylation of the base following an original reaction mechanism that doesn't involve the hydroxyl radical (116). This reaction takes place within 600 fs (Figure 8).

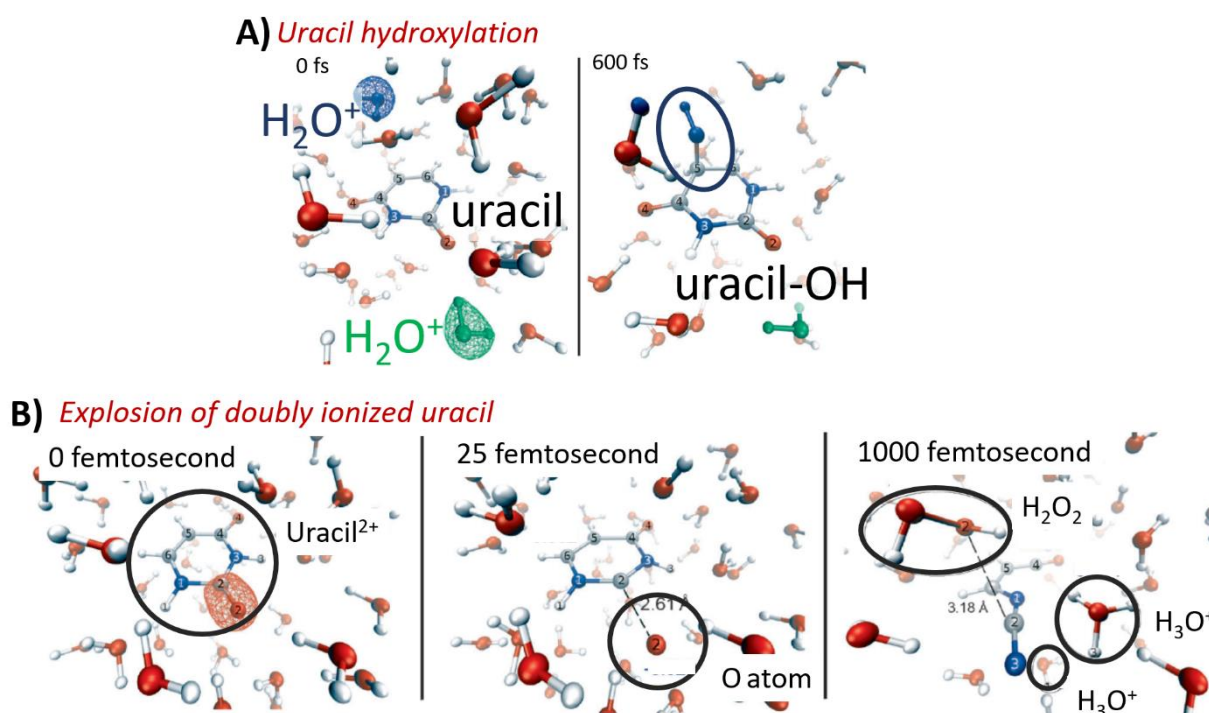


Figure 8: Hydroxylation of the solvated uracil by H_2O^+ formed in its solvation shell (Top) and Coulomb explosion after double ionization. Adapted with permission from ((116)).

In a series of papers, Tavernelli and co-workers explored the consequences of double ionizations of bio-relevant molecules (water, riboses, uracil) (104–107). Double ionization is not a probable event upon proton or alpha-particle irradiation. It is comparatively much more probable with irradiation by heavier ions C^{6+} (90). In any case, if it occurs, double ionization can lead to dramatic consequences for the structural integrity of ionized molecules. Indeed, the number of negative charges held by electrons is generally not sufficient to compensate anymore the repulsive interactions among atom nuclei and a so-called Coulomb explosion can take place. An example is provided in Figure 8B in the case of uracil.

CONCLUSION AND PERSPECTIVES

This review was intended to portray the state of the art of first-principles simulations dedicated to the first stages of biological matter radiolysis. After having recalled some of the currently opened questions regarding the formation of radiation damage by direct effects and low-energy electrons,

as well as the new opportunities brought by the advent of attosecond science, we have highlighted some recently proposed methodologies dedicated to the modelling of the physical and physical-chemical stages. Most applications have dealt with small gas phase molecules or small solvated molecules, far from the complex biological structures shown in Figure 1. Nevertheless, applications of RT-TD-DFT to much larger systems comprised of almost one thousand atoms at the DFT level are now accessible with various codes, attesting progress in the field and opening exciting perspectives for more realistic simulations.

We have drawn attention to some aspects that from our point of view are still unsatisfactorily treated. The issue of electronic decoherence is certainly a major one as it limits the horizon of applicability of RT-TD-DFT beyond the very first femtoseconds after irradiation. Another one is the need to further develop interpretative tools to analyse the outcomes of the simulations and to extract insights that can be understood within the well-established vocabulary of radiation chemistry.

We have focused on the shortest stages of irradiation. Clearly it will be necessary to bridge the gap to longer time scales. Integrative multiscale methods should be developed in the future. Although the road to reach fully realistic modelling of biological matter radiolysis is still a long and winding one, we hope we have convinced the reader, that it is a thrilling research field with uncountable opportunities for young researchers.

DISCLOSURE STATEMENT

The authors are not aware of any affiliation, memberships, funding or financial holdings that might be perceived as affecting the objectivity of this review.

SUMMARY POINTS

1. We have summarized the hallmarks of irradiation by ionizing radiation and have described the multiscale responses of biological molecules subjected to IoR. Current open questions are related to the complicated molecular mechanisms of clustered damage formation in DNA, proteins or protein/DNA complexes, and also the diffusion and reactivity of secondary electrons in natural biological structures. We have finally stressed the opportunities offered by attosecond spectroscopies to help unravel the earliest stages of radiolysis that, up to now, remained inaccessible to standard pulsed radiolysis set-ups.

2. We have shown that Real-Time Time-Dependent DFT is emerging as a promising approach to simulate energy deposition by charged particles in materials and in realistic DNA models. Already insights into the mechanisms of hole formation, subsequent charge migrations and localization of secondary electrons could be obtained. We also have stressed some points that will deserve more in-depth analyses and benchmarks.
3. We have reviewed the simulations carried out by various research groups to address the difficulties of modelling of dissociative electron attachment by first-principles dynamics approaches. Still we have recalled results from other groups suggesting that nucleobase environment strongly impacts the dissociation channels energy landscape.
4. We have shown that Ehrenfest MD simulations have a great potential to reveal unexpected chemical reactivity taking place on the sub-picosecond time scale after irradiation. So, while most studies addressed small biomolecules in water, they pave the way for applications to more complex biological structures.

FUTURE ISSUES

1. Computational efficiency needs to be further pushed forward dramatically to really embrace the complexity of IoR damage, notably clustered damages. An objective of a few thousands up to ten thousand atoms seems to be a good target. This is a challenging, but probably a reachable target for TD-DFT based approaches within the very next years.
2. Extending the types of ionizing particles in RT-TD-DFT, to include low-energy electrons, positrons, muons, but also γ -rays, X-rays and other the electrons-photons coupled channels (e.g. Auger emission).
3. More validation of the outcomes of RT-TD-DFT simulations against experimental data from attosecond spectroscopies, on small and large systems, are needed. The reliability of adiabatic and non-adiabatic XC functionals for radiation chemistry problems needs to be fully clarified, as well as the issues arising from self-interaction-error on charge migrations.
4. Conceptual tools to characterize secondary electrons produced in RT-TDDFT simulations need to be invented. For example, to evaluate their kinetic energies and their angular scattering, and also to investigate the diffusion of low energy electrons.
5. Electronic decoherence needs to be incorporated for large molecular systems.

6. Applications to larger and more realistic models of macro-biomolecules should be envisioned step-by-step.

ACKNOWLEDGEMENTS

We kindly thank Xiaojing Wu, Xiaodong Zhao, Angela Parise and Aurelio Alvarez-Ibarra for their contributions to results reviewed in this article, as well as to our collaborators for many enlightening discussions. Financial support was provided by CNRS (Project Emergence@INC 2018) and the French *Agence Nationale de la Recherche* (Project RUBI, number: ANR-19-CE29-0011-01). We are grateful for GENCI (project A0060706913) and to Compute Canada for providing us with generous computational resources.

CITED LITERATURE

1. Sklodowska Curie M. 1904. *Recherches sur les Substances Radioactives*. Thèse de docteur en sciences physiques thesis. Faculté des Sciences de Paris
2. Hatano Y, Katsumura Y, Mozumder A. 2010. Introduction. In *Charged Particle and Photon Interactions with Matter*, pp. 1–7. CRC Press
3. Dizdaroglu M, Jaruga P. 2012. Mechanisms of free radical-induced damage to DNA. *Free Radic. Res.* 46(4):382–419
4. Yamamori T, Yasui H, Yamazumi M, Wada Y, Nakamura Y, et al. 2012. Ionizing radiation induces mitochondrial reactive oxygen species production accompanied by upregulation of mitochondrial electron transport chain function and mitochondrial content under control of the cell cycle checkpoint. *Free Radic. Biol. Med.* 53(2):260–70
5. Yoshida T, Goto S, Kawakatsu M, Urata Y, Li T. 2012. Mitochondrial dysfunction, a probable cause of persistent oxidative stress after exposure to ionizing radiation. *Free Radic. Res.* 46(2):147–53
6. Szumiel I. 2015. Ionizing radiation-induced oxidative stress, epigenetic changes and genomic instability: The pivotal role of mitochondria. *Int. J. Radiat. Biol.* 91(1):1–12
7. Huber S, Butz L, Stegen B, Klumpp D, Braun N, et al. 2013. Ionizing radiation, ion transports, and radioresistance of cancer cells. *Front. Physiol.* 4:212

8. Stark G. 2005. Functional Consequences of Oxidative Membrane Damage. *J. Membr. Biol.* 205(1):1–16
9. Cucinotta FA, Durante M. 2006. Cancer risk from exposure to galactic cosmic rays: implications for space exploration by human beings. *Lancet Oncol.* 7(5):431–35
10. Kuncic Z, Lacombe S. 2018. Nanoparticle radio-enhancement: principles, progress and application to cancer treatment. *Phys. Med. Biol.* 63(2):02TR01
11. Kamada T, Tsujii H, Blakely EA, Debus J, De Neve W, et al. 2015. Carbon ion radiotherapy in Japan: an assessment of 20 years of clinical experience. *Lancet Oncol.* 16(2):e93–100
12. Lacombe S, Porcel E, Scifoni E. 2017. Particle therapy and nanomedicine: state of art and research perspectives. *Cancer Nanotechnol.* 8(1):9
13. Lorat Y, Brunner CU, Schanz S, Jakob B, Taucher-Scholz G, Rübe CE. 2015. Nanoscale analysis of clustered DNA damage after high-LET irradiation by quantitative electron microscopy – The heavy burden to repair. *DNA Repair.* 28:93–106
14. Sage E, Shikazono N. 2017. Radiation-induced clustered DNA lesions: Repair and mutagenesis. *Oxidative DNA Damage Repair.* 107:125–35
15. Mavragani IV, Nikitaki Z, Souli MP, Aziz A, Nowsheen S, et al. 2017. Complex DNA Damage: A Route to Radiation-Induced Genomic Instability and Carcinogenesis. *Cancers.* 9(7):
16. Kakarougkas A, Jeggo PA. 2014. DNA DSB repair pathway choice: an orchestrated handover mechanism. *Br. J. Radiol.* 87(1035):20130685
17. Asaithamby A, Hu B, Chen DJ. 2011. Unrepaired clustered DNA lesions induce chromosome breakage in human cells. *Proc. Natl. Acad. Sci.*, p. 201016045
18. Lukas J, Lukas C, Bartek J. 2011. More than just a focus: The chromatin response to DNA damage and its role in genome integrity maintenance. *Nat Cell Biol.* 13(10):1161–69
19. Wilson MD, Benlekhir S, Fradet-Turcotte A, Sherker A, Julien J-P, et al. 2016. The structural basis of modified nucleosome recognition by 53BP1. *Nature.* 536:100
20. Boudaïffa B, Cloutier P, Hunting D, Huels MA, Sanche L. 2000. Resonant Formation of DNA Strand Breaks by Low-Energy (3 to 20 eV) Electrons. *Science.* 287(5458):1658
21. Elahe Alizadeh, Thomas M. Orlando, Léon Sanche. 2015. Biomolecular Damage Induced by Ionizing Radiation: The Direct and Indirect Effects of Low-Energy Electrons on DNA. *Annu. Rev. Phys. Chem.* 66(1):379–98

22. Dong Y, Gao Y, Liu W, Gao T, Zheng Y, Sanche L. 2019. Clustered DNA Damage Induced by 2–20 eV Electrons and Transient Anions: General Mechanism and Correlation to Cell Death. *J. Phys. Chem. Lett.* 10(11):2985–90
23. Ma J, Wang F, Denisov SA, Adhikary A, Mostafavi M. 2017. Reactivity of prehydrated electrons toward nucleobases and nucleotides in aqueous solution. *Sci. Adv.* 3(12):e1701669
24. Ma J, Kumar A, Muroya Y, Yamashita S, Sakurai T, et al. 2019. Observation of dissociative quasi-free electron attachment to nucleoside via excited anion radical in solution. *Nat. Commun.* 10(1):102
25. Arumainayagam CR, Garrod RT, Boyer MC, Hay AK, Bao ST, et al. 2019. Extraterrestrial prebiotic molecules: photochemistry vs. radiation chemistry of interstellar ices. *Chem. Soc. Rev.* 48(8):2293–2314
26. Bennett CJ, Pirim C, Orlando TM. 2013. Space-Weathering of Solar System Bodies: A Laboratory Perspective. *Chem. Rev.* 113(12):9086–9150
27. Nass K. 2019. Radiation damage in protein crystallography at X-ray free-electron lasers. *Acta Crystallogr. Sect. D.* 75(2):211–218
28. Bury C, Garman EF, Ginn HM, Ravelli RBG, Carmichael I, et al. 2015. Radiation damage to nucleoprotein complexes in macromolecular crystallography
29. Loh Z-H, Doumy G, Arnold C, Kjellsson L, Southworth SH, et al. 2020. Observation of the fastest chemical processes in the radiolysis of water. *Science.* 367(6474):179
30. Trinter F, Schöffler MS, Kim H-K, Sturm FP, Cole K, et al. 2014. Resonant Auger decay driving intermolecular Coulombic decay in molecular dimers. *Nature.* 505(7485):664–66
31. Calegari F, Ayuso D, Trabattoni A, Belshaw L, De Camillis S, et al. 2014. Ultrafast electron dynamics in phenylalanine initiated by attosecond pulses. *Science.* 346(6207):336
32. Belloni J, Monard H, Gobert F, Larbre J-P, Demarque A, et al. 2005. ELYSE—A picosecond electron accelerator for pulse radiolysis research. *Nucl. Instrum. Methods Phys. Res. Sect. Accel. Spectrometers Detect. Assoc. Equip.* 539(3):527–39
33. Thürmer S, Ončák M, Ottosson N, Seidel R, Hergenbahn U, et al. 2013. On the nature and origin of dicationic, charge-separated species formed in liquid water on X-ray irradiation. *Nat. Chem.* 5(7):590–96
34. Dinh PM, du Bourg LB, Gao C-Z, Gu B, Lacombe L, et al. 2017. On the Quantum Description of Irradiation Dynamics in Systems of Biological Relevance. In *Nanoscale Insights*

into *Ion-Beam Cancer Therapy*, ed AV Solov'yov, pp. 277–309. Cham: Springer International Publishing

35. Kohanoff J, McAllister M, Tribello GA, Gu B. 2017. Interactions between low energy electrons and DNA: a perspective from first-principles simulations. *J. Phys. Condens. Matter.* 29(38):383001
36. Gu J, Leszczynski J, Schaefer HF. 2012. Interactions of Electrons with Bare and Hydrated Biomolecules: From Nucleic Acid Bases to DNA Segments. *Chem. Rev.* 112(11):5603–40
37. Monari A, Dumont E. 2015. Understanding DNA under oxidative stress and sensitization: the role of molecular modeling. *Front. Chem.* 3:43
38. Tavernelli I. 2015. Nonadiabatic Molecular Dynamics Simulations: Synergies between Theory and Experiments. *Acc. Chem. Res.* 48(3):792–800
39. Parise A, Alvarez-Ibarra A, Wu X, Zhao X, Pilmé J, de la Lande A. 2018. Quantum Chemical Topology of the Electron Localization Function in the Field of Attosecond Electron Dynamics. *J. Phys. Chem. Lett.*, pp. 844–50
40. Howell RW. 2008. Auger processes in the 21st century. *Int. J. Radiat. Biol.* 84(12):959–75
41. Cederbaum LS, Zobeley J, Tarantelli F. 1997. Giant Intermolecular Decay and Fragmentation of Clusters. *Phys. Rev. Lett.* 79(24):4778–81
42. Sonntag C von. 2010. Radiation-Induced DNA Damage: Indirect Effects. In *Recent Trends in Radiation Chemistry*, pp. 543–62. WORLD SCIENTIFIC
43. Becker D, Adhikary A, Sevilla MD. 2010. Mechanisms of Radiation-Induced DNA Damage: Direct Effects. In *Recent Trends in Radiation Chemistry*, pp. 509–42. WORLD SCIENTIFIC
44. LaVere T, Becker D, Sevilla MD. 1996. Yields of OH· in gamma-irradiated DNA as a function of DNA hydration: Hole transfer in competition OH· formation. *Radiat Res.* 145:673
45. Cederbaum LS, Zobeley J. 1999. Ultrafast charge migration by electron correlation. *Chem. Phys. Lett.* 307(3):205–10
46. Friedland W, Dingfelder M, Kunderát P, Jacob P. 2011. Track structures, DNA targets and radiation effects in the biophysical Monte Carlo simulation code PARTRAC. *Chem. DNA Damage Repair Biol. Significance Comprehending Future.* 711(1):28–40

47. Francis Z, Incerti S, Karamitros M, Tran HN, Villagrasa C. 2011. Stopping power and ranges of electrons, protons and alpha particles in liquid water using the Geant4-DNA package. *12th Int. Conf. Nucl. Microprobe Technol. Appl.* 269(20):2307–11
48. Marante C, Klinker M, Corral I, González-Vázquez J, Argenti L, Martín F. 2017. Hybrid-Basis Close-Coupling Interface to Quantum Chemistry Packages for the Treatment of Ionization Problems. *J. Chem. Theory Comput.* 13(2):499–514
49. Jagau T-C, Bravaya KB, Krylov AI. 2017. Extending Quantum Chemistry of Bound States to Electronic Resonances. *Annu. Rev. Phys. Chem.* 68(1):525–53
50. Miteva T, Kazandjian S, Sisourat N. 2017. On the computations of decay widths of Fano resonances. *Electrons Nucl. Motion - Correl. Dyn. Mol. Occas. 70th Birthd. Lorenz Cederbaum.* 482:208–15
51. Whitenack DL, Wasserman A. 2011. Density Functional Resonance Theory of Unbound Electronic Systems. *Phys. Rev. Lett.* 107(16):163002
52. Runge E, Gross EKH. 1984. Density-Functional Theory for Time-Dependent Systems. *Phys. Rev. Lett.* 52(12):997–1000
53. Calvayrac F, Reinhard PG, Suraud E. 1995. Nonlinear plasmon response in highly excited metallic clusters. *Phys. Rev. B.* 52(24):R17056–59
54. Yabana K, Bertsch GF. 1996. Time-dependent local-density approximation in real time. *Phys. Rev. B.* 54(7):4484–87
55. Flick J, Ruggenthaler M, Appel H, Rubio A. 2015. Kohn–Sham approach to quantum electrodynamical density-functional theory: Exact time-dependent effective potentials in real space. *Proc. Natl. Acad. Sci.* 112(50):15285
56. Wu X, Alvarez-Ibarra A, Salahub DR, de la Lande A. 2018. Retardation in electron dynamics simulations based on time-dependent density functional theory. *Eur. Phys. J. D.* 72(12):206
57. Rizzi V, Todorov TN, Kohanoff JJ. 2017. Inelastic electron injection in a water chain. *Sci. Rep.* 7(1):45410
58. Schild A, Gross EKH. 2017. Exact Single-Electron Approach to the Dynamics of Molecules in Strong Laser Fields. *Phys. Rev. Lett.* 118(16):163202

59. Zhao L, Tao Z, Pavošević F, Wildman A, Hammes-Schiffer S, Li X. 2020. Real-Time Time-Dependent Nuclear-Electronic Orbital Approach: Dynamics beyond the Born-Oppenheimer Approximation. *J. Phys. Chem. Lett.* 11(10):4052–58
60. Castro A, Marques MAL, Rubio A. 2004. Propagators for the time-dependent Kohn-Sham equations. *J. Chem. Phys.* 121(8):3425–33
61. Gómez Pueyo A, Marques MAL, Rubio A, Castro A. 2018. Propagators for the Time-Dependent Kohn-Sham Equations: Multistep, Runge-Kutta, Exponential Runge-Kutta, and Commutator Free Magnus Methods. *J. Chem. Theory Comput.* 14(6):3040–52
62. A. Schleife, E. W. Draeger, V. M. Anisimov, A. A. Correa, Y. Kanai. 2014. Quantum Dynamics Simulation of Electrons in Materials on High-Performance Computers. *Comput. Sci. Eng.* 16(5):54–60
63. Andrade X, Strubbe D, De Giovannini U, Larsen AH, Oliveira MJT, et al. 2015. Real-space grids and the Octopus code as tools for the development of new simulation approaches for electronic systems. *Phys. Chem. Chem. Phys.* 17(47):31371–96
64. Kühne TD, Iannuzzi M, Del Ben M, Rybkin VV, Seewald P, et al. 2020. CP2K: An electronic structure and molecular dynamics software package - Quickstep: Efficient and accurate electronic structure calculations. *J. Chem. Phys.* 152(19):194103
65. Köster AM, Reveles JU, del Campo JM. 2004. Calculation of exchange-correlation potentials with auxiliary function densities. *J. Chem. Phys.* 121(8):3417–24
66. Dunlap BI, Rösch N, Trickey SB. 2010. Variational fitting methods for electronic structure calculations. *Mol. Phys.* 108(21–23):3167–80
67. The deMon developers. *deMon2k*
68. Mejía-Rodríguez D, Köster AM. 2014. Robust and efficient variational fitting of Fock exchange. *J. Chem. Phys.* 141(12):124114
69. Delesma FA, Geudtner G, Mejía-Rodríguez D, Calaminici P, Köster AM. 2018. Range-Separated Hybrid Functionals with Variational Fitted Exact Exchange. *J. Chem. Theory Comput.* 14(11):5608–16
70. de la Lande A, Clavaguéra C, Köster A. 2017. On the accuracy of population analyses based on fitted densities#. *J. Mol. Model.* 23(4):99
71. de la Lande A, Alvarez-Ibarra A, Hasnaoui K, Cailliez F, Wu X, et al. 2019. Molecular Simulations with in-deMon2k QM/MM, a Tutorial-Review. *Molecules.* 24(9):

72. Wu X, Teuler J-M, Cailliez F, Clavaguéra C, Salahub DR, de la Lande A. 2017. Simulating Electron Dynamics in Polarizable Environments. *J. Chem. Theory Comput.* 13(9):3985–4002
73. Li X, Tully JC, Schlegel HB, Frisch MJ. 2005. Ab initio Ehrenfest dynamics. *J. Chem. Phys.* 123(8):084106
74. Tavernelli * I, Röhrig UF, Rothlisberger U. 2005. Molecular dynamics in electronically excited states using time-dependent density functional theory. *Mol. Phys.* 103(6–8):963–81
75. Schleife A, Kanai Y, Correa AA. 2015. Accurate atomistic first-principles calculations of electronic stopping. *Phys. Rev. B.* 91(1):014306
76. *Electronic Stopping Power of Matter for Ions*. Nuclear Data Section of the International Atomic Energy Agency. <https://www-nds.iaea.org>
77. Ziegler JF. *The Stopping and Range of Ions in Matter*. <http://srim.org>
78. Mozumder A, Hatano Y. 2004. *Charged Particle and Photon Interactions with Matter*. Boca Raton: ., CRC Press ed.
79. Shukri AA, Bruneval F, Reining L. 2016. Ab initio electronic stopping power of protons in bulk materials. *Phys. Rev. B.* 93(3):035128
80. Maliyov I, Crocombette J-P, Bruneval F. 2020. Quantitative electronic stopping power from localized basis set. *Phys. Rev. B.* 101(3):035136
81. Correa AA. 2018. Calculating electronic stopping power in materials from first principles. *Comput. Mater. Sci.* 150:291–303
82. Yost DC, Yao Y, Kanai Y. 2017. Examining real-time time-dependent density functional theory nonequilibrium simulations for the calculation of electronic stopping power. *Phys. Rev. B.* 96(11):115134
83. Yu HS, Li SL, Truhlar DG. 2016. Perspective: Kohn-Sham density functional theory descending a staircase. *J. Chem. Phys.* 145(13):130901
84. Fuks JI, Lacombe L, Nielsen SEB, Maitra NT. 2018. Exploring non-adiabatic approximations to the exchange–correlation functional of TDDFT. *Phys. Chem. Chem. Phys.* 20(41):26145–60
85. Ullrich CA, Yang Z. 2014. A Brief Compendium of Time-Dependent Density Functional Theory. *Braz. J. Phys.* 44(1):154–88
86. Dinh PM, Lacombe L, Reinhard P-G, Suraud É, Vincendon M. 2018. On the inclusion of dissipation on top of mean-field approaches. *Eur. Phys. J. B.* 91(10):246

87. Privett AJ, Teixeira ES, Stopera C, Morales JA. 2017. Exploring water radiolysis in proton cancer therapy: Time-dependent, non-adiabatic simulations of $H^+ + (H_2O)_1-6$. *PLOS ONE*. 12(4):e0174456
88. Reeves KG, Kanai Y. 2017. Electronic Excitation Dynamics in Liquid Water under Proton Irradiation. *Sci. Rep.* 7(1):40379
89. Yost DC, Kanai Y. 2019. Electronic Excitation Dynamics in DNA under Proton and α -Particle Irradiation. *J. Am. Chem. Soc.* 141(13):5241–51
90. Alvarez-Ibarra A, Parise A, Hasnaoui K, de la Lande A. 2020. The physical stage of radiolysis of solvated DNA by high-energy-transfer particles: insights from new first principles simulations. *Phys. Chem. Chem. Phys.* 22(15):7747–58
91. A. Trabattoni, M. Galli, M. Lara-Astiaso, A. Palacios, J. Greenwood, et al. 2019. Charge migration in photo-ionized aromatic amino acids. *Philos. Trans. R. Soc. Math. Phys. Eng. Sci.* 377(2145):20170472
92. Lara-Astiaso M, Galli M, Trabattoni A, Palacios A, Ayuso D, et al. 2018. Attosecond Pump–Probe Spectroscopy of Charge Dynamics in Tryptophan. *J. Phys. Chem. Lett.* 9(16):4570–77
93. Andrea Rozzi C, Maria Falke S, Spallanzani N, Rubio A, Molinari E, et al. 2013. Quantum coherence controls the charge separation in a prototypical artificial light-harvesting system. *Nat. Commun.* 4(1):1602
94. Vacher M, Bearpark MJ, Robb MA, Malhado JP. 2017. Electron Dynamics upon Ionization of Polyatomic Molecules: Coupling to Quantum Nuclear Motion and Decoherence. *Phys. Rev. Lett.* 118(8):083001
95. Polyak I, Jenkins AJ, Vacher M, Bouduban MEF, Bearpark MJ, Robb MA. 2018. Charge migration engineered by localisation: electron-nuclear dynamics in polyenes and glycine. *Mol. Phys.* 116(19–20):2474–89
96. Nijjar P, Jankowska J, Prezhdo OV. 2019. Ehrenfest and classical path dynamics with decoherence and detailed balance. *J. Chem. Phys.* 150(20):204124
97. Min SK, Agostini F, Tavernelli I, Gross EKV. 2017. Ab Initio Nonadiabatic Dynamics with Coupled Trajectories: A Rigorous Approach to Quantum (De)Coherence. *J. Phys. Chem. Lett.* 8(13):3048–55

98. Cai Z, Chen S, Wang L-W. 2019. Dissociation path competition of radiolysis ionization-induced molecule damage under electron beam illumination. *Chem. Sci.* 10(46):10706–15
99. Geerlings P, Chamorro E, Chattaraj PK, De Proft F, Gázquez JL, et al. 2020. Conceptual density functional theory: status, prospects, issues. *Theor. Chem. Acc.* 139(2):36
100. Chauvin R, Lepetit C, Silvi B, Alikhani E. *Applications of Topological Methods in Molecular Chemistry*, Vol. 22. Springer, Cham ed.
101. Pilmé J, Luppi E, Bergès J, Houée-Lévin C, de la Lande A. 2014. Topological analyses of time-dependent electronic structures: application to electron-transfers in methionine enkephalin. *J. Mol. Model.* 20(8):2368
102. Burnus T, Marques MAL, Gross EKV. 2005. Time-dependent electron localization function. *Phys. Rev. A.* 71(1):010501
103. Schnitker J, Rossky PJ. 1987. Quantum simulation study of the hydrated electron. *J. Chem. Phys.* 86(6):3471–85
104. Cédric Nicolas, Anne Boutin, Bernard Lévy, Daniel Borgis. 2003. Molecular simulation of a hydrated electron at different thermodynamic state points. *J. Chem. Phys.* 118(21):9689–96
105. Savolainen J, Uhlig F, Ahmed S, Hamm P, Jungwirth P. 2014. Direct observation of the collapse of the delocalized excess electron in water. *Nat. Chem.* 6(8):697–701
106. Li X, Sevilla MD, Sanche L. 2003. Density Functional Theory Studies of Electron Interaction with DNA: Can Zero eV Electrons Induce Strand Breaks? *J. Am. Chem. Soc.* 125(45):13668–69
107. Schyman P, Laaksonen A. 2008. On the Effect of Low-Energy Electron Induced DNA Strand Break in Aqueous Solution: A Theoretical Study Indicating Guanine as a Weak Link in DNA. *J. Am. Chem. Soc.* 130(37):12254–55
108. Chen H-Y, Yang P-Y, Chen H-F, Kao C-L, Liao L-W. 2014. DFT Reinvestigation of DNA Strand Breaks Induced by Electron Attachment. *J. Phys. Chem. B.* 118(38):11137–44
109. Li X, Sanche L, Sevilla MD. 2006. Base Release in Nucleosides Induced by Low-Energy Electrons: A DFT Study. *Radiat. Res.* 165(6):721–29
110. Kumar A, Becker D, Adhikary A, Sevilla MD. 2019. Reaction of Electrons with DNA: Radiation Damage to Radiosensitization. *Int. J. Mol. Sci.* 20(16):
111. Smyth M, Kohanoff J. 2011. Excess Electron Localization in Solvated DNA Bases. *Phys. Rev. Lett.* 106(23):238108

112. McAllister M, Smyth M, Gu B, Tribello GA, Kohanoff J. 2015. Understanding the Interaction between Low-Energy Electrons and DNA Nucleotides in Aqueous Solution. *J. Phys. Chem. Lett.* 6(15):3091–97
113. Gu B, Smyth M, Kohanoff J. 2014. Protection of DNA against low-energy electrons by amino acids: a first-principles molecular dynamics study. *Phys. Chem. Chem. Phys.* 16(44):24350–58
114. Marsalek O, Elles CG, Pieniazek PA, Pluhařová E, VandeVondele J, et al. 2011. Chasing charge localization and chemical reactivity following photoionization in liquid water. *J. Chem. Phys.* 135(22):224510
115. Wang F, Schmidhammer U, de La Lande A, Mostafavi M. 2017. Ultra-fast charge migration competes with proton transfer in the early chemistry of H_2O^+ . *Phys. Chem. Chem. Phys.* 19(4):2894–99
116. López-Tarifa P, Gageot M-P, Vuilleumier R, Tavernelli I, Alcamí M, et al. 2013. Ultrafast Damage Following Radiation-Induced Oxidation of Uracil in Aqueous Solution. *Angew. Chem. Int. Ed.* 52(11):3160–63
117. López-Tarifa P, Penhoat M-AH du, Vuilleumier R, Gageot M-P, Tavernelli I, et al. 2012. Ultrafast non-adiabatic fragmentation dynamics of doubly charged uracil in gas and liquid phase. *J. Phys. Conf. Ser.* 388(10):102055
118. López-Tarifa P, Hervé du Penhoat M-A, Vuilleumier R, Gageot M-P, Tavernelli I, et al. 2011. Ultrafast Nonadiabatic Fragmentation Dynamics of Doubly Charged Uracil in a Gas Phase. *Phys. Rev. Lett.* 107(2):023202
119. Hervé du Penhoat M-A, Moraga NR, Gageot M-P, Vuilleumier R, Tavernelli I, Politis M-F. 2018. Proton Collision on Deoxyribose Originating from Doubly Ionized Water Molecule Dissociation. *J. Phys. Chem. A.* 122(24):5311–20
120. López-Tarifa P, Grzegorz D, Piekarski, Rossich E, Penhoat M-AH du, et al. 2014. Ultrafast nonadiabatic fragmentation dynamics of biomolecules. *J. Phys. Conf. Ser.* 488(1):012037